Utilization of One-dimensional Raman Spectroscopy for the Investigation into Transport Phenomena between Supercritical Carbon Dioxide Sessile Bubble and Liquid Solvent Environment

Jaypee Quino[*1,2], Philipp Hackner[1,2], and Andreas Braeuer[1,2]

[1]Lehrstuhl für Technische Thermodynamik (LTT), Friedrich-Alexander Universität Erlangen-Nürnberg, Am Weichselgarten 8, 91058 Erlangen, Germany

[2]Erlangen Graduate School in Advanced Optical Technologies (SAOT), Friedrich-Alexander Universität Erlangen-Nürnberg, Paul-Gordan-Str. 6, 91052 Erlangen, Germany

*Jaypee.Quino@aot.uni-erlangen.de, Fax: +49 9131 8525851

ABSTRACT

The knowledge of mass transport quantities is crucial for the optimization, scale-up and design of supercritical (sc) fluid-based technologies. Unfortunately, the capability of determining these quantities remains a serious challenge due to experimental complexity. In order to develop a measurement strategy extracting this information, the setup can be simplified into the analysis of single drops and/or single bubbles of fluids in a compressed binary mixture system. This would eventually provide further simplifications such as symmetry and wide control of parameters.

In this contribution, we report a procedure to generate and to perform in situ composition measurements involving sc carbon dioxide (CO_2) sessile bubble in a liquid solvent environment. The CO_2 has initially been conditioned above its critical state and subsequently introduced into the chamber as a sc sessile bubble. The chamber which is initially filled with ethanol prior to the introduction of sessile bubble has also been conditioned at the same temperature and pressure of the sessile bubble but below their mixture critical pressure (MCP). By controlling the pump feed flows and regulators, the bubble progresses and reaches a hemispherical geometry before departure from the glass capillary tip. This hemispherical geometry has been assumed as the steady-state condition for which the analysis has been carried out. With the help of Raman spectroscopy which is a non-invasive technique, spatially resolved composition profiles could be quantified which lead to the derivation of mass transport quantities.

INTRODUCTION

The economical, environmental-friendly and mild characteristics of supercritical (sc) carbon dioxide (CO_2) has enabled it to become a potential alternative to conventional process technology routes - from food processing using sc extraction and separation processes [1-4] to polymer-based applications using sc CO_2 as a foaming agent [5-8]. Such processes are accompanied with nucleation, bubble formation and bubble growth of the sc fluid component. These bubbles are able to interact with their solvent surrounding through an interfacial layer, which acts as a site for mass transportation. Hence, in order to truly benefit from the use of sc fluid-based technology, the ability to analyze the mass transport mechanisms that govern the process is of utmost importance for its optimization, scale-up and design. This is rather challenging though in extreme conditions, transient phenomenon and with limited optical access. Nevertheless, the complexity can be reduced by investigating single drops or single bubbles as a pilot study. Here, we investigate sc CO_2 bubbles in liquid solvent environment. As a preliminary step, an organic solvent composed of ethanol has been used in this study instead of a polymer compound. Upon the utilization of Raman spectroscopy the composition profiles inside and outside of the bubble could be accessed in-situ which enables us to distinguish the phases and phase boundaries.

MATERIALS AND METHODS

Bubbles of carbon dioxide (CO_2) have been generated in ethanol solvent environment. Both CO_2 and ethanol were used in this study without further treatment. CO_2, with 99.5% purity was obtained from Linde (Germany) while ethanol was purchased from Merck KGaA (Germany) with 99.9% purity. As described in Figure 1, CO_2 bubbles are generated inside the high pressure chamber equipped with temperature and pressure sensors and electrical heating elements. Prior to the introduction of bubbles, the chamber is pressurized with neat ethanol above the critical pressure (73.8 bar) of CO_2 and heated above the CO_2 critical temperature (31.1°C). CO_2 is then fed into the chamber pre-heated with the same temperature as that of the solvent but at slightly higher pressure (~1-2 bar) to induce pressure gradient for flow of CO_2. A syringe suction pump connected to the chamber exit (not shown in the diagram) compensates the pressure difference and therefore plays a key role in regulating the pressure and minimizing bubble fluctuations. This leads to the formation of sessile bubbles of CO_2 at the tip of the glass capillary featuring an internal diameter of 1.6 mm and wall thickness of 0.7 mm.

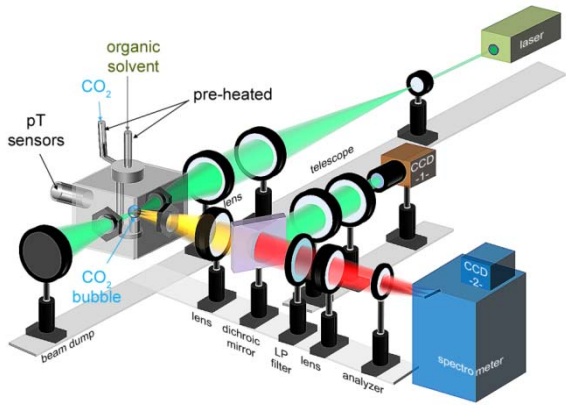

Figure 1: Sketch of the optically accessible high-pressure chamber with the capillary system to generate qusi-static sc CO2 sessile bubbles in liquid solvent environment and the measurement configurations

We describe in the same Figure 1 the Raman measurement procedure (refer to [9] for details). The excitation source is a continuous-wave frequency-doubled Nd:YVO4 laser operated at 532 nm wavelength and laser power of 2.0 W. The initial beam diameter is expanded by means of a Galilean telescope. The collimated beam is then focused at the center of the chamber where CO_2 bubble is situated. Close to the focal point of the laser forms a thin cylinder positioned through the center of bubble. From this line-shape one-dimensional measurement volume, light is scattered into all spatial directions. An achromatic lens located perpendicular to the excitation axis is used to collect these scattered signals. The elastically-scattered light component is reflected by means of a dichroic mirror while the Raman-scattered signal is transmitted for analysis. This elastically-scattered light, recorded by the charge-coupled device (CCD) camera 1, is used for visualization to ensure that line-imaging is performed through the center of the bubble.

Meanwhile, the corresponding Raman-scattered signals are focused spatially-resolved into the entrance slit of an imaging spectrometer. Such type of spectrometer conserves the spatial information along the probe volume as detected by CCD camera 2. The imaging mechanism facilitates simultaneous recording of spectra from 40 measurement points along the sessile bubble at a single time instant.

RESULTS

Figure 2 illustrates how the Raman signals originating from the one-dimensional measurement volume (Figure 2a) are detected spectrally and spatially resolved on one CCD chip (Figure 2b). The spatial axis of the detector consists of 400 pixel rows. A trade-off between signal-to-noise ratio and spatial resolution has existed after combining 10 pixel rows to form 10 superpixel rows, resulting in a spatial resolution of the one dimensional measurement volume of 60 μm. Because of the weak CO_2 signal inside the bubble, we have chosen the evaluation range close to the Fermi dyads of CO_2 where ethanol signature (represented by CH_3 asymmetric deformation/bend) of comparable intensity exists. This is at the range between 1161 cm^{-1} and 1557 cm^{-1} wavenumbers. In Figure 2c, the exemplary Raman spectra at two local points reveal the exclusive presence of neat CO_2 inside the bubble, while the coexistence of both the CO_2 and ethanol occurs outside of the bubble.

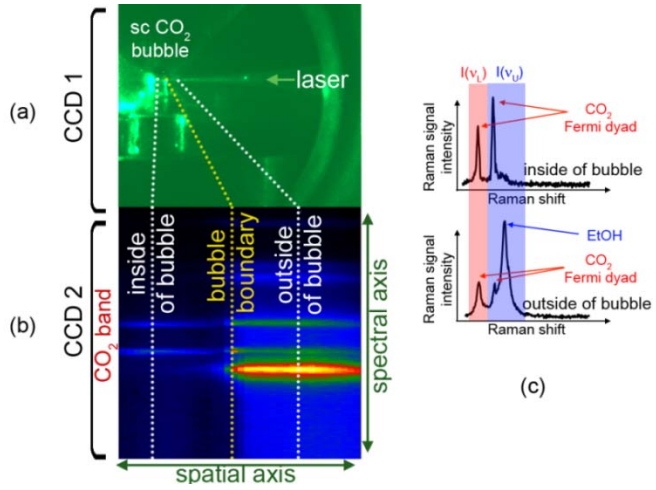

Figure 2: Illustration showing how Raman signals originating from the probe volume are detected spectrally- and spatially-resolved with a single charge-coupled device (CCD) chip. Exemplary Raman spectra at selected regions are shown for comparison.

In order to interpret the recorded Raman spectra, two spectral regions have to be evaluated which are $I(\nu_L)$ band between 1161 cm^{-1} and 1320 cm^{-1} and $I(\nu_U)$ band between 1320 cm^{-1} to 1557 cm^{-1} representing the respective locations of lower and upper levels of CO_2 Fermi resonance. A special consideration regarding the integrated Raman signal intensities of the mentioned bands allows the system to be calibrated.

We assumed the system in all our experiments to be axisymmetric, and thus we only have to analyze half of the bubble. In Figure 3, the acquired Raman signal intensities are plotted together with the measured mole fractions of a sc CO_2 bubble at 76.74 bar and 50.2°C. The normalized intensities in grayscale bar (left) define the shape of the bubble which is proportional to the number of scatterers, and thereby allows us to identify the outer layer of the bubble. Complementary to the normalized intensity, the mole fraction of CO_2 in colored-scale bar (right) identifies the phases along the probed line based on the binary phase diagram of the set conditions.

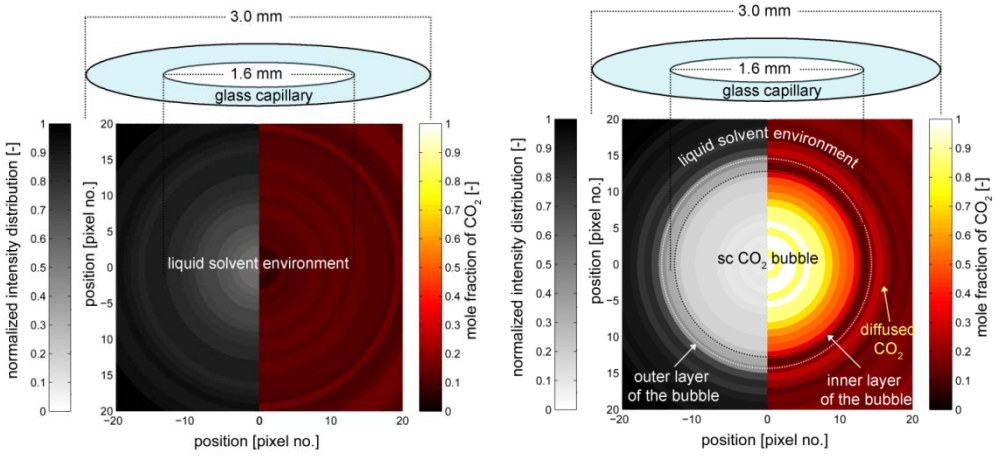

Figure 3: Measured normalized Raman signal intensity distribution and mole fraction (a) before the occurrence, and (b) at steady-state regime of sc CO2 bubble. The bubble is bounded by an interfacial mixing layer. The actual dimension of the capillary is shown as inset.

Figure 3a reveals that before the occurrence of sc CO_2 bubble, the environment is in a liquid phase. The derived mole fraction of CO_2 of around 0.1 implies that a small amount of CO_2 has diffused and has been detected 1 mm above the tip of the capillary. The bubble progresses and reaches a hemispherical geometry before departure from the glass capillary tip. This hemispherical geometry has been assumed as the quasi-steady-state condition for which the analysis has been carried out (see Figure 3b). The profile of sc CO_2 bubble is recognized by the normalized intensities and mole fraction of CO_2. In addition, an interfacial layer is identified which is bounded by the saturation mole fraction of the CO_2-ethanol mixture and the extremum slope of the integrated Raman signal intensities. In this layer, a portion of CO_2 diffuses out of the bubble through the layer while at the same time, the ethanol evaporates.

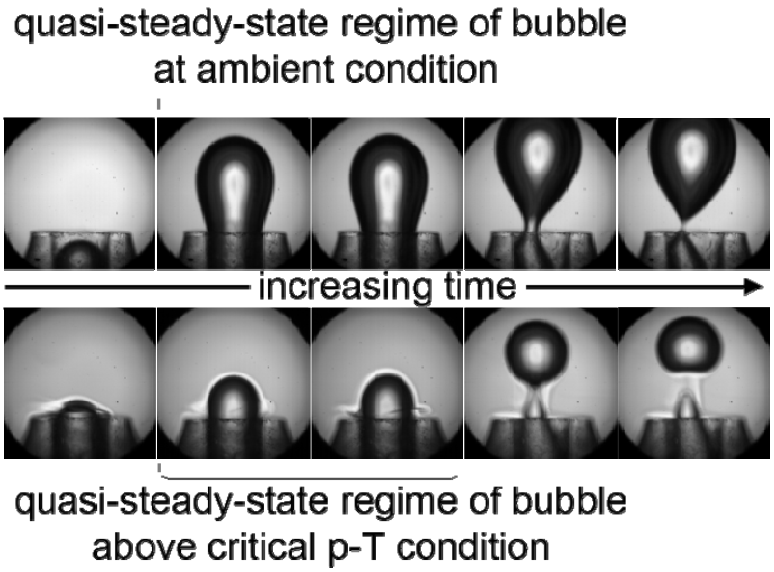

Figure 4: Comparison of bubble evolution (top) at ambient conditions and (bottom) above the critical pressure and temperature. Quasi-steady state regimes are emphasized.

Besides the Raman measurements, we performed shadowgraph experiments to visualize the time evolution of bubbles generated at ambient condition and above the critical conditions of CO_2. As expected, CO_2 bubbles generated at higher pressures are smaller compared to at ambient conditions as shown in Figure 4. The quasi-steady-state regime which is important for the analysis is highlighted. Shadowgraph images confirm the refractive index gradient between the bubble and the solvent environment which can be attributed to the thin interfacial layer that permits the CO_2 to diffuse into and the ethanol to evaporate.

CONCLUSION

We have demonstrated a procedure to generate sc CO_2 bubbles in ethanol solvent environment. Raman spectroscopy has been applied to monitor the composition profile of sc CO_2 bubbles. Both the Raman measurements and shadowgraph images recognize an interfacial layer that surrounds the bubble. The saturation mole fraction of CO_2-ethanol mixture, which is temperature dependent, defines the inner boundary while the integrated Raman intensity defines the outer layer. Therefore, the accurate thickness of the layer will only be identified if the real temperatures inside, outside and at the interface are known.

ACKNOWLEDGEMENT

The authors gratefully acknowledge financial support for parts of this work by the German Research Foundation (DFG) which additionally funds the Erlangen Graduate School in Advanced Optical Technologies (SAOT) in the framework of the German excellence initiative.

REFERENCES

[1] BRUNNER, G., J. Food Eng., Vol. 67, **2005**, p. 21-33

[2] WANG, L., WELLER, C., Trends Food Sci. Technol., Vol. 17, **2006**, p. 300-312

[3] LANG, Q., WAI, C., Talanta, Vol. 53, **2001**, p. 771-782

[4] SHIMODA, M., ISHIKAWA, H., KAWANO, T., OSAKIMA, J. Food Sci., Vol. 59, **1994**, p. 231-233

[5] GOEL, S., BECKMANN, E., Polym. Eng. Sci., Vol. 34, **1994**, p. 1137-1147

[6] SAUCEAU, M., FAGES, J., COMMON, A., NIKITINE, C. RODIER, E., Prog. Polym. Sci., Vol. 36, **2011**, p. 749-766

[7] KAZARIAN, S. G., Polym. Sci., Ser. C., Vol. 42, **2000**, p. 78-101

[8] SHUKLA, S., KOELLING, K., Ind. Eng. Chem. Res., Vol. 48, **2009**, p. 7603-7615

[9] BRAEUER, A., KNAUER, O.S., QUINO, J., LEIPERTZ, A., Int. J. Heat Mass Transf., Vol. 62, **2013**, p. 729-740